Journal of Magnetism and Magnetic Materials ∎ (∎∎∎∎) ∎∎∎–∎∎∎

Contents lists available at ScienceDirect

Journal of Magnetism and Magnetic Materials

journal homepage: www.elsevier.com/locate/jmmm

Charge ordering in $Nd_{2/3}Ca_{1/3}MnO_3$: ESR and magnetometry study

D.M. Polishchuk [a], A.I. Tovstolytkin [a], E.L. Fertman [b,*], V.A. Desnenko [b], O. Kravchyna [b], D.D. Khalyavin [c], A.N. Salak [d], A.G. Anders [e], A. Feher [f]

[a] Institute of Magnetism of NASU, 36b Vernadsky Boulevard, Kyiv 03680, Ukraine
[b] B. Verkin Institute for Low Temperature Physics and Engineering of NASU, 47 Lenin Ave., Kharkov 61103, Ukraine
[c] ISIS Facility, STFC, Rutherford Appleton Laboratory, Chilton, Didcot, Oxfordshire OX11 0QX, UK
[d] Department of Materials and Ceramic Engineering/CICECO, University of Aveiro, Aveiro 3810-193, Portugal
[e] V. N. Karazin Kharkiv National University, 4 Svobody sq., Kharkiv 61000, Ukraine
[f] Institute of Physics, Faculty of Science, P. J. Šafárik University in Košice, Park Angelinum 9, Košice 04154, Slovakia

ARTICLE INFO

Article history:
Received 8 September 2015
Received in revised form
2 March 2016
Accepted 4 March 2016

Keywords:
Manganites
Electron-spin resonance
Charge ordering
Phase separation
Static magnetization

ABSTRACT

The evolution of magnetic and electric properties of the narrow-band manganite $Nd_{2/3}Ca_{1/3}MnO_3$ was studied by the electron-spin resonance (ESR), static magnetic field (dc) and resistivity techniques in the temperature range of 100–380 K. It was found that below the charge ordering temperature, $T_{CO} \approx 212$ K, the compound is a mixture of the charge ordered and charge disordered phases in varying proportions depending on the temperature. The exchange phase process, when the amount of the charge ordered phase increases under cooling, while the amount of the charge disordered phase decreases is the most intense between ~220 K and 180 K. At low temperatures, $T < 160$ K, the charge ordered to the charge disordered phase ratio is about 4:1, which is in excellent agreement with previous neutron diffraction data. Both a sharp decrease of the magnetic susceptibility and a huge resistivity increase are evident of the weakening of ferromagnetic correlations and suppression of the double exchange interaction across the charge ordering due to the localization of the charge carriers.

© 2016 Published by Elsevier B.V.

1. Introduction

Among the currently known magnetic materials magnetic oxides play a special role due to their unique physical properties and practical application. Mixed valence manganites are widely studied in the past two decades because of the effect of colossal magnetoresistance (CMR) [1–3]. Such compounds with a general formula $R_{1-x}M_xMnO_3$ (where R and M are a rare earth and a divalent elements, respectively), containing two types of ions, Mn^{3+} and Mn^{4+}, in a ratio which is determined by the concentration of divalent element x, crystallize in a perovskite structure. Exotic properties of these compounds are determined by a strong coupling between magnetic, charge and lattice degrees of freedom. It was found that many of these compounds are single-phase above room temperature, but they become spontaneously phase separated when cooled below this temperature, and represent more or less dispersed mixture of two or more phases, which differ in crystal structure, electronic structure, magnetic properties. Phase separation phenomena play a key role in the physics of this class of materials [3–6]. Mechanisms of the spontaneous phase separation are still not fully understood, that does not permit to control the process by means of the external factors, such as temperature, magnetic field or pressure.

Charge ordering (CO) tightly connected with phase separation is one of the most interesting phenomena observed in mixed valence manganites. The CO implies the real space ordering of the Mn^{3+} and Mn^{4+} ions which occurs on cooling below a certain temperature, T_{CO}. As charge plays an important role in the exchange coupling in such compounds, the CO is expected to induce an anomaly in the magnetic behavior of the compound. In a narrow band $Nd_{2/3}Ca_{1/3}MnO_3$ CMR perovskite the charge ordering takes place at T_{CO}~212 K [7]. The results of our previous studies are consistent with its martensitic scenario. Martensitic phase transformations are diffusionless collective phase transitions of the first-order type leading to the coexistence of high-temperature and low-temperature phases in a wide temperature range. Such transformation proceeds via an atomic rearrangement that involves a collective shear displacement. It is accompanied by the development of the phase segregated state in a wide temperature range, in which the high temperature crystal phase and the low temperature one coexist. On cooling, the growing low temperature phase induces stress (so-called accommodation strains) to other regions of the same crystallite, preventing them from transformation. As a result, further cooling is needed for further growth of the martensitic phase. It is assumed that cooling of

* Corresponding author.

http://dx.doi.org/10.1016/j.jmmm.2016.03.022
0304-8853/© 2016 Published by Elsevier B.V.

UNCORRECTED PROOF

$Nd_{2/3}Ca_{1/3}MnO_3$ below T_{CO} leads to a coexistence of the low-temperature charge-ordered and the residual charge-disordered phases similar to that reported in Ref. [8]. Further cooling results in a magnetic phase separation as the charge-ordered domains become antiferromagnetic, while the residual charge-disordered phase stabilized by accommodation stresses becomes a ferromagnetic one [9]. A series of successive magnetic phase transitions was found by neutron diffraction study. On cooling, $Nd_{2/3}Ca_{1/3}MnO_3$ undergoes two antiferromagnetic transitions at 130 K and 80 K, and a ferromagnetic one at 60 K [10,11]. It leads to the antiferromagnetic (AFM) – ferromagnetic (FM) phase separated state at low temperatures. The exchange bias effect recently found is evident of the AFM – FM phase separated state as well [12].

In this work, we report on the electron-spin-resonance (ESR), static magnetic field (dc) and resistivity studies of $Nd_{2/3}Ca_{1/3}MnO_3$. The electron-spin-resonance is a useful tool for studying phase diagrams of complex magnetic materials both in the paramagnetic regime (normal ESR) [13–15] and in the mode of magnetic ordering (ferromagnetic resonance, FMR) [16,17]. A significant advantage of the ESR technique is a good sensitivity to both magnetic and structural inhomogeneity [18,19]. It allows us to study the magnetic multiphase state, what is not always possible with other techniques [20]. The present study is aimed to contribute to understanding of spontaneous phase separation in complex oxides.

2. Experimental details

The $Nd_{2/3}Ca_{1/3}MnO_3$ ceramics were prepared by a standard solid state reaction technique from the stoichiometric amounts of the respective oxides [21]. The ESR studies were carried out over 100–380 K using an X-band ELEXSYS E500 EPR spectrometer in the *X*- and *K*-band (f=9.46 GHz and 24.3 GHz, respectively) on the ceramic and powder samples. The ceramic sample was prepared as a cylinder with both diameter and height of about 3 mm. The powder sample was prepared from the ceramic one by grinding. A characteristic particle size of the powder sample was below 0.1 mm.

Magnetic measurements were made using the Quantum Design Magnetic Properties Measurement System (MPMS) and a non-commercial superconducting quantum interference device (SQUID) magnetometer at various applied magnetic fields up to 50 kOe in the temperature range of 2–300 K. Resistivity measurements were done using a standard four-point technique at a frequency of 30 Hz in the 100–300 K temperature range.

3. Results

3.1. Dc magnetization and resistivity study: the ferromagnetic correlations across the charge ordering

Temperature dependent $M(T)$ curves for $Nd_{2/3}Ca_{1/3}MnO_3$ measured in external magnetic fields of H=0.02–50 kOe demonstrate a pronounced shoulder in the vicinity of the charge ordering transformation, T_{CO}~212 K (Inset in Fig. 1). In paramagnetic state (above T_N~130 K), the temperature dependent inverse dc magnetic susceptibility curves $1/\chi$ measured in all the applied magnetic fields are seen to coincide both above and below T_{CO} (Fig. 1). The external magnetic fields up to 50 kOe do not affect the charge ordering temperature. The $1/\chi$ (T) curves change their slope across the charge ordering. The paramagnetic Curie temperatures are defined as Θ_1~132 K in the 225–255 K temperature range and Θ_2 ~90 K in the 140–195 K range. The positive Curie temperatures are evident of the ferromagnetic correlations both above and

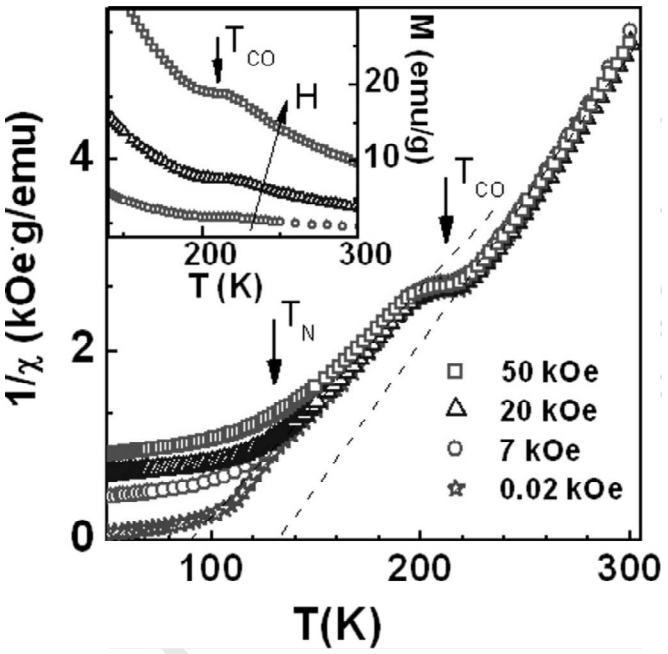

Fig. 1. Temperature dependent inverse dc magnetic susceptibility $1/\chi$ (T) measured in different magnetic fields. Inset: temperature dependent dc magnetization $M(T)$ in different magnetic fields.

below T_{CO}. Decrease of the Θ value across the charge ordering implies the weakening of the ferromagnetic correlations, resulting in a drop of the susceptibility. It is associated with a suppression of the double exchange interaction due to the localization of the charge carriers and well agrees with temperature dependent resistivity behavior.

Fig. 2 shows the temperature dependence of resistivity for $Nd_{2/3}Ca_{1/3}MnO_3$. It can be seen that the resistivity shows a semiconductor-like transport behavior, and increases steeply around T_{CO}~212 K, which is defined as corresponding peak of the resistivity derivative (Inset in Fig. 2). The resistivity changes about three orders of magnitude when cooling from 300 K to 150 K.

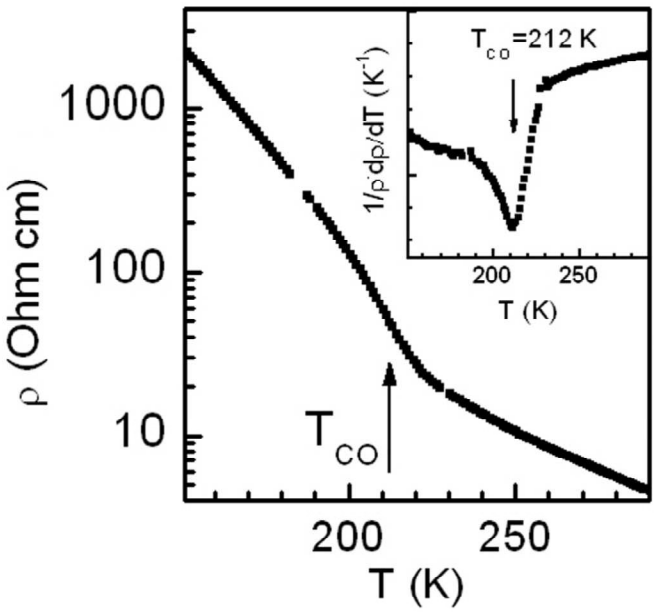

Fig. 2. Temperature dependence of the resistivity for $Nd_{2/3}Ca_{1/3}MnO_3$ measured at 30 Hz. Inset: the temperature dependence of the derivative of resistivity around T_{CO}.

UNCORRECTED

Please cite this article as: D.M. Polishchuk, et al., Journal of Magnetism and Magnetic Materials (2016), http://dx.doi.org/10.1016/j.jmmm.2016.03.022

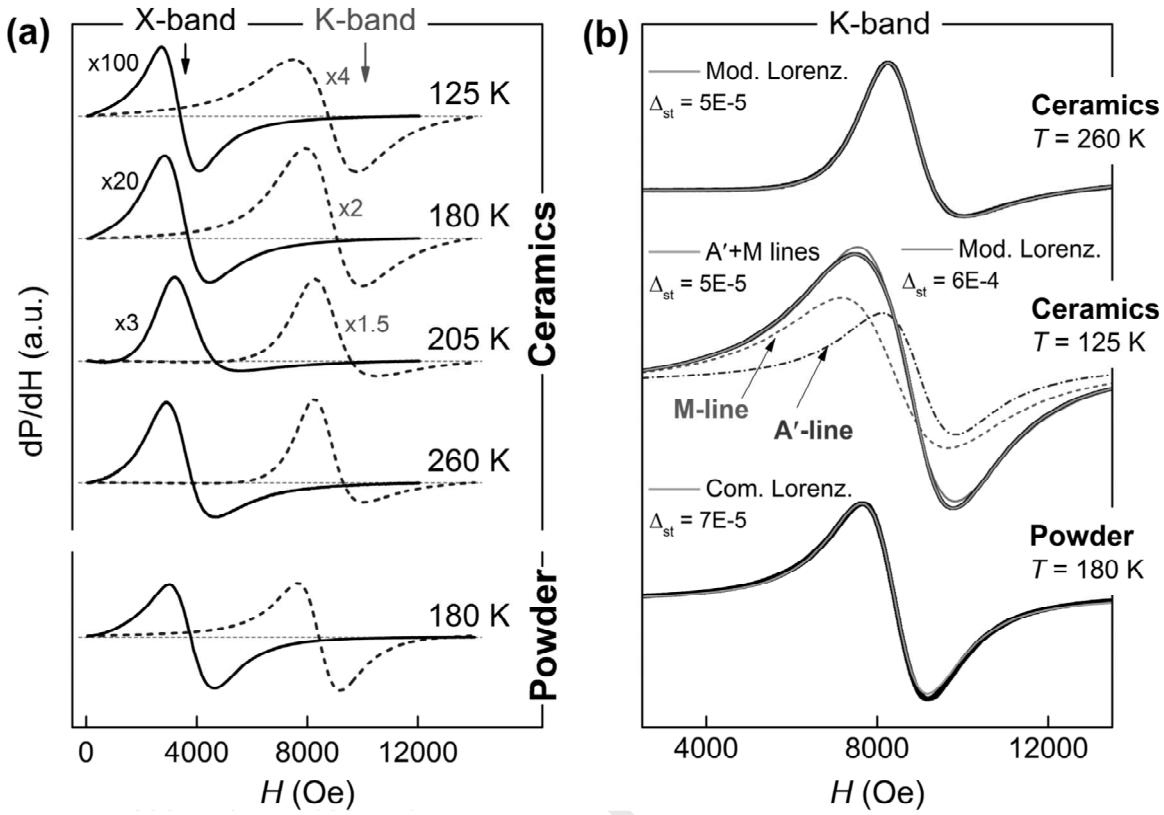

Fig. 3. (a) The ESR spectra for the ceramic and powder $Nd_{2/3}Ca_{1/3}MnO_3$ samples obtained in the *X*-and *K*-frequency bands at different temperatures. The resonant lines of the ceramic sample are shown both for the temperatures above and below $T_{CO} \approx 212$ K. (b) Examples of the different fitting of the experimental ESR spectra: the fitting using one Lorentzian curve (thin solid lines in the upper and lower graphs) and comparison of the fitting using one or two Lorentzian curves (thin solid lines in the middle graph; for the case of two Lorentzians the fitted curve coincides with the experimental one). The dotted and dash-dotted lines in the middle graph are the two components of the summary curve.

3.2. ESR spectra

Fig. 3a shows the characteristic curves of the ESR absorption spectra obtained from the magnetic resonance studies of both the ceramic and powder $Nd_{2/3}Ca_{1/3}MnO_3$ samples in the *X*-and *K*-frequency bands at different temperatures. A single resonance line with a linewidth of the order of the resonance field value is observed for both samples. The resonance field value corresponds to the g-factor value $g \approx 2$ [19].

The ESR lines for the ceramic sample are asymmetric relative to the zero line (horizontal dotted lines in Fig. 3a) in both frequency bands. The degree and character of the asymmetry are dependent on temperature. An attentive look at the ESR spectra allows one to distinguish three temperature ranges with different ESR line shapes: (1) $T > T_{CO}$; (2) $T < T_{CO}$; (3) $T \sim T_{CO}$. These features will be discussed in more detail below. The resonance line for powder sample is symmetrical over the entire temperature range under study.

3.3. ESR spectra processing

The observed asymmetry of the ESR lines may be caused by two reasons: (i) the dispersion effects due to the presence of conductive regions [13,22], (ii) the existence of two (or more) phases with different resonant characteristics [20]. The results of the *X*-and *K*-frequency band experiments taken separately cannot unambiguously suggest which of the options is valid. However, the comparison of these results with each other and with those obtained for the powder sample allows one to come to a firm conclusion that at $T > T_{CO}$ the option (i) is valid, while at $T < T_{CO}$ the option (ii) is realized (see Section 4 for details).

At the first stage, the Dysonian derivative line is chosen as a fitting curve for the analysis of the spectra [22]:

$$\frac{dP}{dH} = \frac{d}{dH}\left(A\left[\frac{\Delta H + \alpha(H - H_{res})}{4(H - H_{res})^2 + \Delta H^2} + \frac{\Delta H - \alpha(H + H_{res})}{4(H + H_{res})^2 + \Delta H^2}\right]\right), \quad (1)$$

where ΔH is the half-width of the resonance line, H_{res} is resonance field, A is the area under the absorption curve, α is asymmetry coefficient, which is the dispersion to the absorption ratio [23,24]. Generally, the second term in Eq. (1) can be neglected, but not in the case of $\Delta H \sim H_{res}$ [22].

In the particular cases when the experimental data can be successfully fitted using the first term in Eq. (1) only, the fit line is called a modified Lorentzian. In addition, if the line is symmetric ($\alpha = 0$), it is called a common Lorentzian.

Fig. 3b shows the fitting results (solid lines) of the experimental ESR spectra using Eq. (1) at several temperatures. At $T > T_{CO}$, all the resonance lines both for *X*- and *K*-bands are well described by a single line (Eq. (1)); a standard deviation Δ_{st} of the spectra normalized to the height of the first peak is about 10^{-5}. However, at $T < T_{CO}$ the *K*-band resonance curve of the ceramic sample appeared to be better described by two lines (Eq. (1)). Central graph of Fig. 3b compares the results of the fitting of the experimental ESR spectra at $T = 125$ K with one or two Lorentzian curves. In the latter case, the $\Delta_{st} \sim 10^{-5}$, which is much less then $\Delta_{st} \sim 10^{-4}$ for the fitting by a single line. The validity of this two-line approach, which is initially based on *mathematical* considerations, will be substantiated by (i) the results of a rigorous analysis of the ESR spectra evolution and (ii) broad discussion of the features of the manifestation of CO phenomena in magnetic and resonance properties of manganites (see details in Section 4), which will lie

Please cite this article as: D.M. Polishchuk, et al., Journal of Magnetism and Magnetic Materials (2016), http://dx.doi.org/10.1016/j.jmmm.2016.03.022

Table 1
The parameters obtained by magnetometry and ESR techniques.

	T, K	$C^{(a)}$, $\frac{K\cdot emu}{Oe\cdot g}$	$\Theta_{CW}{}^{(a)}$, K	$g_{eff}{}^{(b)}$	$\Delta H_\infty{}^{(c)}$, kOe	$\Theta_{esr}{}^{(d)}$, K	ρ, Ohm cm	$\delta^{(e)}$, mm
1	$T>240$	0.031	132	2.021	6.3(5.35)	135	~1	0.5(0.3)
2	$150<T<210$	0.042	90	2.026	5.55(4.75)	90	~1000	16.4(10.2)

firm and unambiguous *physical* foundation for the above description of the underlying processes.

Below, the analysis of the results is organized as follows. First ESR data are analyzed on the assumption that over the entire temperature range the ESR spectrum consists of a single asymmetric absorption line. This approach allows selecting the temperature regions with identical ESR spectra characteristics and determining the ranges of abnormal behavior. Then an attention is focused on the analysis of the *K*-band spectra as they proved to be more informative. It is shown that at $T<T_{CO}$ the single-line approach encounters a number of difficulties. For this reason, the spectra at $T<T_{CO}$ are decomposed into two resonance absorption lines and detailed analysis of the temperature dependent parameters of each of these lines is done.

4. Discussion

4.1. X-band ESR spectra for the ceramic $Nd_{2/3}Ca_{1/3}MnO_3$

X-band ESR spectra of the $Nd_{2/3}Ca_{1/3}MnO_3$ ceramic sample have been well fitted by a modified Lorentzian. Fig. 4 shows the temperature dependences of the resonance field H_{res} and linewidth ΔH obtained from the modified Lorentzian fitting. Both dependences demonstrate sharp anomalies in the phase transformation temperature region in the vicinity of $T_{CO}\approx 212$ K. Anomalies of the resonance curves observed below 150 K are evident of the gradual evolution of the resonant properties of the compound caused by the antiferromagnetic phase transition at $T_N\approx 130$ K [10]. The temperature behavior of the ESR linewidth provides information about the degree of the inhomogeneity of the system and a character of its magnetic relaxation [19]. Usually,

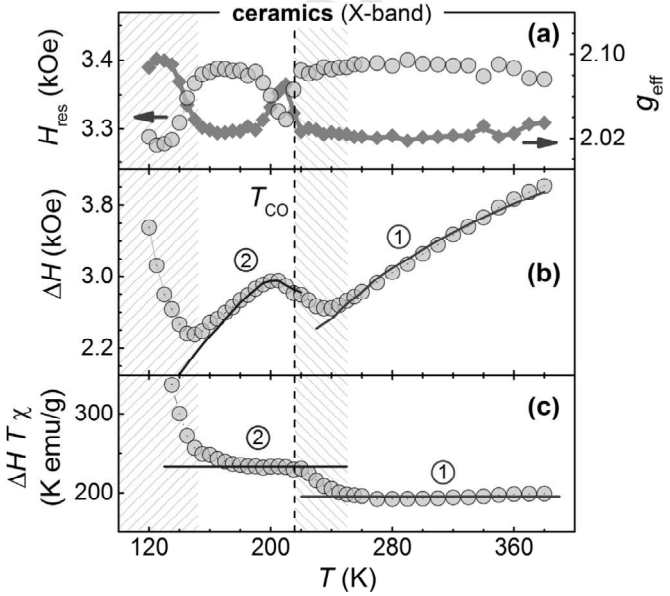

Fig. 4. Temperature dependences of the resonant field $H_{res}(T)$ and effective *g*-factor g_{eff} (a), linewidth $\Delta H(T)$ (b) and $\Delta H\cdot T\cdot\chi(T)$ (c). Solid lines represent fits using the models described in text.

in lanthanum-substituted manganites, the ESR linewidth increases with increasing temperature $T>1.1T_{cr}$ [25,26] which is associated with the spin-phonon relaxation [27,28] (here, T_{cr} is a temperature of a magnetic phase transformation). At the same time, the linewidth grows fast in the vicinity of the magnetic phase transition temperature T_{cr} ($T_{cr}<T\lesssim 1.1T_{cr}$) [25,29]. A similar behavior has been observed in the vicinity of the different phase transformations, such as the ferromagnetic, antiferromagnetic and/or charge-ordering transitions. In the isotropic case, the linewidth can be described by the expression [25]:

$$\Delta H(T)=\frac{C}{T\chi(T)}[K(T)+f(\epsilon)], \tag{2}$$

where *C* is a Curie constant, $\chi(T)$ is magnetic susceptibility, $K(T)$ and $f(\varepsilon)$ (where $\varepsilon=(T-T_{cr})/T_{cr}$) are noncritical and critical contribution to $\Delta H(T)$, respectively. Since the $f(\varepsilon)$ is essential only near T_{cr}, at other temperatures $\Delta H(T)$ is determined by the temperature dependent $K(T)$ only. At $T\gg T_{cr}$, when the spin-spin interaction predominates, $\Delta H(T)$ is $\Delta H_\infty=$const as $T\chi(T)$ becomes equal to *C* and $K(T)=$const [27].

In our case, the effective *g*-factor value, $g\approx 2$ (Fig. 3a), which is close to a free electron value, is evident of the weak spin-orbit interactions and the dominant spin-spin interactions [19]. Then to fit the experimental data for $T\gg T_{cr}$ the Eq. (2) can be written as:

$$\Delta H(T)=\frac{C}{T\chi_{exp}(T)}\Delta H_\infty, \tag{3}$$

where $\chi_{exp}(T)$ is the experimental dependence obtained using the magnetometry technique.

Using the dependence $\Delta H\cdot T\cdot\chi(T)$ we can identify the range of the non-critical behavior of $\Delta H(T)$ described by Eq. (3) and the range of the critical changes described by the second term of Eq. (2). The dependence of $\Delta H\cdot T\cdot\chi(T)$ (Fig. 4c) obtained from the experiment shows two non-critical ranges (marked as 1 and 2) demonstrating linear behavior determined by the Eq. (3), and two critical regions in the vicinity of the charge ordering and magnetic ordering, respectively. $\Delta H\cdot T\cdot\chi(T)$ dependences in the ranges 1 and 2 (Fig. 4c) are well approximated by horizontal lines with parameters $\Delta H_\infty{}^{(1)}\approx 6.3$ kOe and $\Delta H_\infty{}^{(2)}\approx 5.6$ kOe. The Curie constants C_1 and C_2 are calculated from the experimental $\chi(T)$ dependences (Fig. 1). All the obtained parameters are summarized in Table 1. The model $\Delta H(T)$ dependences calculated using Eq. (3) and the obtained parameters (Table 1) are shown as solid lines in Fig. 4b. The model dependences both in the ranges 1 and 2 are in a good agreement with the experimental data (Fig. 4c). It implies that in these temperature ranges the $\Delta H(T)$ dependence is determined by the relaxation processes only. The parameters $\Delta H_\infty{}^{(1)}$ and $\Delta H_\infty{}^{(2)}$ characterize the state of the compound in these temperature ranges [27].

(1) The Curie constants by magnetometry study.
(2) The effective *g*-factor by *X*-band ESR study.
(3) The high-temperature linewidth asymptote values in *X*-band for ceramics and powder samples, $\Delta H_\infty{}^{ceramics}$ and ($\Delta H_\infty{}^{powder}$), correspondingly.
(4) The Curie–Weiss temperatures calculated from ESR $\chi_{esr}{}^{-1}$ (T) dependence (Fig. 7).

UNCORRECTED PROOF

Please cite this article as: D.M. Polishchuk, et al., Journal of Magnetism and Magnetic Materials (2016), http://dx.doi.org/10.1016/j.jmmm.2016.03.022

(5) The skin-layer thickness calculated using the experimental $\rho(T)$ dependence for *X*-band and *K*-band, $\delta_{X\text{-}band}$ and ($\delta_{K\text{-}band}$), correspondingly.

The critical $\Delta H(T)$ behavior in the vicinity of the phase transition is determined by the peculiarities of the transition, and depends on the sample and the experimental parameters; in particularly, on frequency [12]. It should be noted that in the critical temperature ranges the anomalous increase of the ESR line intensity and the deviation of the $\chi(T)$ dependence from the Curie–Weiss law are observed [8,12,30]. The anomalous behavior is usually explained by the appearance of anti-ferromagnetic correlations when approaching magnetic phase transition temperature [8]. In our case, there are two anomalous ranges, namely in the vicinity of $T_{CO}\sim$212 K and in the vicinity of $T_N\sim$130 K. The ferromagnetic correlations found when approaching the charge ordering temperature, T_{CO}, from the high temperature range, are evident of the enhancement of inhomogeneous state in the studied compound. It agrees well with the increasing of the ΔH_∞ value: $\Delta H_\infty{}^{(2)} > \Delta H_\infty{}^{(1)}$. To confirm this suggestion the additional ESR experiments were carried out in the *K*-band range for both the ceramics and the powder samples.

4.2. *K*-band ESR spectra for the ceramic $Nd_{2/3}Ca_{1/3}MnO_3$

As it was discussed in Section 3.3 the possible reasons for the resonance line asymmetry can be either dispersion effects due to the presence of conductive regions or the coexistence of several phases with different magnetic resonant properties. To check these assumptions the ESR experiments have been carried out in a higher frequency range of microwave radiation (*K*-band). The high frequency experiments enhance a resolution of separate ESR resonance lines [1]. All the *K*-band ESR spectra of the $Nd_{2/3}Ca_{1/3}MnO_3$ ceramics were fitted using both (i) a single line and (ii) a superposition of two lines approximations by Eq. (1) (see Section 3.3). Let us discuss the obtained parameters.

Fig. 5 shows the temperature dependent asymmetry parameter α obtained by single line fitting in *X*- and *K*-bands for the $Nd_{2/3}Ca_{1/3}MnO_3$ ceramic sample. According to the Dyson theory [6], the α value is inversely proportional to a skin layer thickness δ at a given frequency *f*. The skin layer thickness is determined by empirical formula $\delta = 503(\rho/\mu_m f)^{1/2}$ where μ_m is a magnetic permeability (for paramagnetic materials $\mu_m \approx 1$), *f* is a frequency and ρ is a resistivity. The average *X*-band and *K*-band skin layer thicknesses, δ_X and δ_K, correspondingly, were estimated using the experimental temperature dependence of the resistivity (Fig. 2). It was found that in the high temperature range ($T > 230$ K) $\delta_X{}^{HT} \approx 1.02$ mm, whereas the ceramic sample characteristic size is about 3 mm. The $\delta_X{}^{HT}$ appeared to be about one order of magnitude less than the low temperature (140 K < *T* < 200 K) skin layer thickness, $\delta_X{}^{LT}$. Besides, the high temperature δ_X is approximately 1.6 times higher than δ_K, which leads to the increase of the asymmetry parameter α with increasing frequency on going from *X*- to *K*-band (Fig. 5). It implies that at $T > 230$ K the line asymmetry is caused by the skin effect. At the same time the line asymmetry in the 200 K < *T* < 230 K temperature range is associated with the charge ordering phase transition at $T_{CO} \approx 212$ K.

Thus the estimations indicate that at high temperatures the resonance lines asymmetry is associated with the skin effect, while at low temperature it is originated from the phase separated state of the compound.

Based on the idea of the coexistence of two phases with different magnetic properties below $T_{CO} \approx 212$ K in $Nd_{2/3}Ca_{1/3}MnO_3$, at $T < T_{CO}$ the *K*-band ESR spectra have been fitted by a sum of two resonance lines, A′ and M, and by a single line A at $T > T_{CO}$ (Fig. 6). The resonance parameters of the two components, A′ and M, appeared to be strongly different. Temperature dependences of the resonant field $H_{res}(T)$ are similar for lines A and M, while it is different for line A′ (Fig. 6a). The M linewidth $\Delta H(T)$ is essentially larger than the A and A′ linewidth (Fig. 6b). The important point observed in the temperature dependent relative intensities $I(T)$ of the lines A′ and M (Fig. 6c) is that the intensities *I* of these two lines redistribute below T_{CO}. This certainly reflects the exchange phase process typical of a martensitic phase transformation. Below the charge ordering temperature the intensity of the M line increases while the intensity of A′ decreases on cooling down to about 160 K. On further cooling the intensities of both lines remain constant (Fig. 6). It is known that the ESR line intensity is

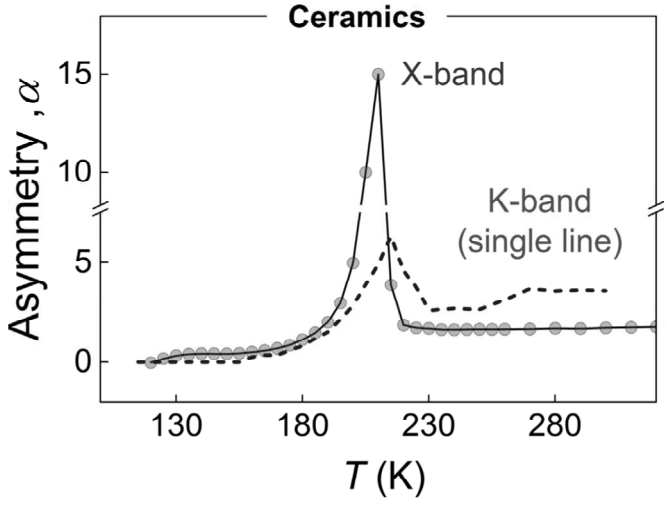

Fig. 5. Temperature dependent asymmetry parameters α obtained by single line fitting in *X*- and *K*-bands for the $Nd_{2/3}Ca_{1/3}MnO_3$ ceramic sample.

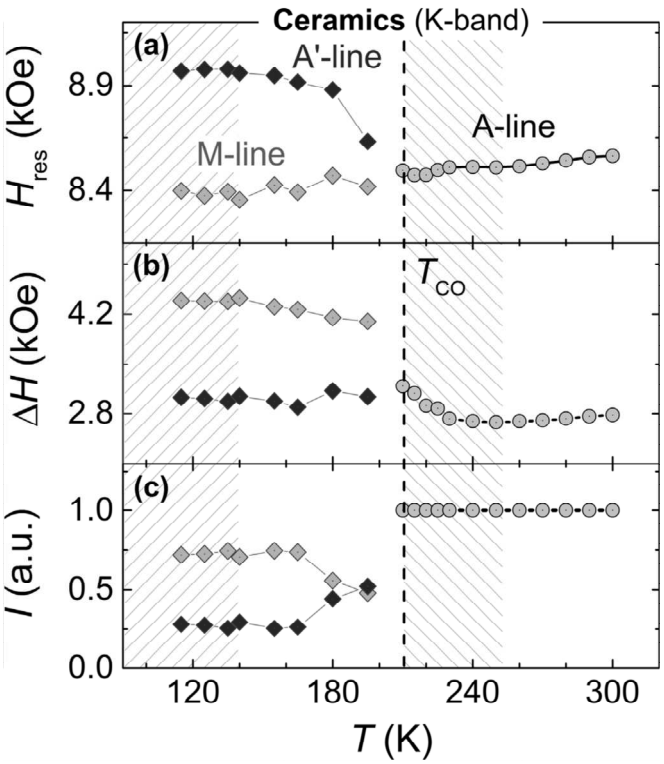

Fig. 6. The temperature dependences of the resonance field $H_{res}(T)$ (a), linewidth $\Delta H(T)$ (b) and relative intensity $I(T)$ (c) of the resonance lines (A, A′ and M) for ceramic $Nd_{2/3}Ca_{1/3}MnO_3$ at *K*-band frequency. The straight solid line (panel a) is a guide for eyes.

Uncorrected Proof

Please cite this article as: D.M. Polishchuk, et al., Journal of Magnetism and Magnetic Materials (2016), http://dx.doi.org/10.1016/j.jmmm.2016.03.022

proportional to both the magnetic susceptibility and the amount of the material under study [1]. Then a redistribution of the intensities between A′ and M lines below T_{CO} implies the redistribution of the phase fractions which correspond to these signals. The line M is associated with the charge-ordered phase and the line A′ is associated with the residual charge-disordered phase which is an excellent agreement with our previous neutron diffraction study and martensitic nature of the charge ordering [7,10,11,31,32]. One should note that this conclusion is in good compliance with the results obtained on other materials exhibiting complex phase separated state. It was shown that the transition into charge ordered phase may not lead to dramatic changes in the resonance field [33,34], but the resonance line of this phase is usually strongly broadened within the whole range of the phase existence [33–35]. On the other hand, the appearance of the correlations of a new phase (either charge ordered or ferromagnetic) within the charge-disordered phase is expected to give rise to noticeable changes in the resonance field of the latter [36].

At low temperature ($T \lesssim 160$ K), the intensities ratio of the A′ and M lines is nearly constant $I_{A'}:I_M \sim 1:4$. Since the magnetizations of both phases are very close, one can expect that the ratio of the volume fractions of the corresponding phases is near 1:4. This is in a good agreement with neutron diffraction data which provide evidence of the coexistence of the charge disordered residual FM phase and the charge ordered AFM phases in the same ratio at low temperatures [11]. A broadening of the M line compared to the A and A′ ones indicates a greater degree of inhomogeneity of the charge-ordered regions which is associated with the martensitic non equilibrium mechanism of their formation driven by internal stresses. The phase redistribution reflects a martensitic kinetics of the charge ordering which is the most intense in the 220–160 K temperature range. The charge ordered phase predominates below 160 K, thus determining the properties of the compound; in particular, a reduction of its magnetic susceptibility (see Fig. 1).

4.3. ESR spectra for the powder $Nd_{2/3}Ca_{1/3}MnO_3$

In order to eliminate the influence of the skin effect on the ESR spectra, a powder sample was studied both in the *X*- and *K*-bands. All the obtained ESR spectra are symmetrical in the whole temperature range of $110 < T < 300$ K that indicates that the role of the skin effect has become negligible. The experimental spectra were approximated by a single common Lorentzian line (Section 3.3). The temperature dependent resonance field, linewidth and spectra intensity obtained for the powder sample in the *K*-band are shown in Figs. 7a, b and 8, respectively. The obtained resonance field

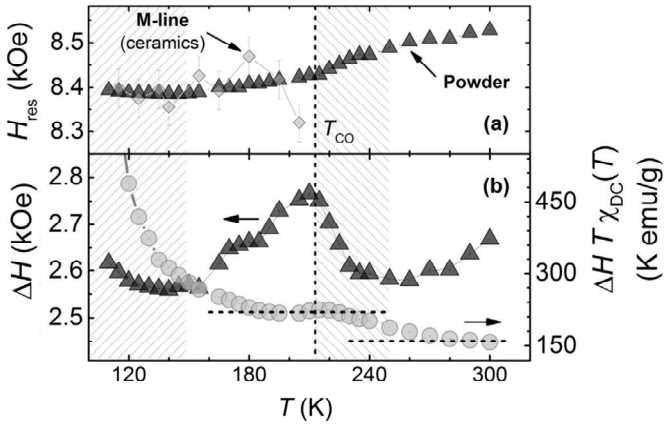

Fig. 7. Temperature dependent (a) resonance field H_{res}, (b) linewidth ΔH and the $\Delta H \cdot T \cdot \chi$ obtained in the *K*-band for powder sample. The diamond symbols (panel (a)) represent $H_{res}(T)$ of the resonance M line for the ceramic sample. The dotted lines (panel (b)) are linear fits for the non-critical regions Eq. (3).

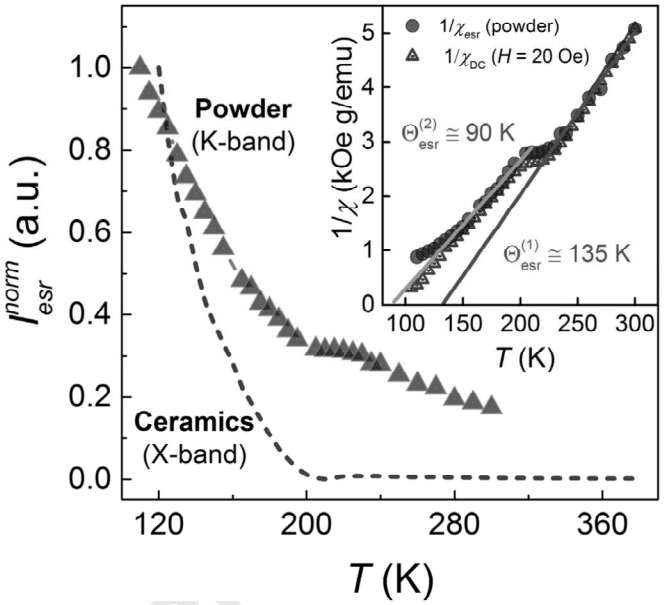

Fig. 8. Temperature dependent normalized ESR intensity $I^{norm}(T)$ for powder (*K*-band) and ceramic (*X*-band) samples. The inset shows the dependences $I^{-1}(T)$ and $\chi^{-1}(T)$. The solid lines are linear fits.

values for the powder and ceramic $Nd_{2/3}Ca_{1/3}MnO_3$ samples are in excellent agreement (Fig. 7a). Both the powder sample and ceramic samples demonstrate anomalies of the linewidth $\Delta H(T)$ and the line intensity $I(T)$ dependences evident of the phase transition in the vicinity of T_{CO}. The temperature dependence of $\Delta H \cdot T \cdot \chi$ is characterized by non-critical and critical regions similar to those discussed earlier for the ceramic sample (Section 4.1). These facts imply that $Nd_{2/3}Ca_{1/3}MnO_3$ undergoes the charge ordering phase transition in the vicinity of $T_{CO} \approx 212$ K regardless of ceramic or powder ($d \leq 0.1$ mm) formes.

All the ESR spectra for the powder sample are symmetrical which does not imply a superposition of two different signals. It has been found that the powder *K*-band resonance line cannot be uniquely fitted by a sum of two lines as it was done for the ceramics. At the same time, the temperature dependence of the intensity, $I(T)$, for the powder sample differs from the one for the ceramic sample: it is less abrupt in the charge ordered state (Fig. 8). Furthermore, the temperature dependent inverse intensity $I^{-1}(T)$ corresponds well to the temperature dependent inverse dc magnetic susceptibility $\chi^{-1}(T)$ at $T > 150$ K (Fig. 8, inset). The critical temperatures $\Theta_{esr}^{(1)} \approx 135$ K and $\Theta_{esr}^{(2)} \approx 90$ K, obtained from the ESR dependences $I^{-1}(T)$ are in excellent agreement with the paramagnetic Curie temperatures $\Theta_1 \sim 132$ K and $\Theta_2 \sim 90$ K obtained by the magnetometry technique. The difference in the ESR spectra for the ceramic and powder samples is associated with the different level of their internal stresses. The charge ordering phase transition is a fundamental property of $Nd_{2/3}Ca_{1/3}MnO_3$, it takes place in near $T_{CO} \approx 212$ K both for the ceramic or powder samples. It leads to the abrupt weakening of the ferromagnetic correlations on cooling across T_{CO} due to the localization of the charge carriers and a suppression of the double exchange interaction.

5. Conclusions

In summary, we have studied the temperature behavior of $Nd_{2/3}Ca_{1/3}MnO_3$ across the charge ordering transition using the electron-spin resonance, static magnetic field and resistivity techniques. All the characteristics obtained, the ESR parameters, magnetic susceptibility and resistivity, demonstrate clear

UNCORRECTED PROOF

Please cite this article as: D.M. Polishchuk, et al., Journal of Magnetism and Magnetic Materials (2016), http://dx.doi.org/10.1016/j.jmmm.2016.03.022

anomalies evident of the charge ordering phase transition near $T_{CO} \approx 212$ K. The electron spin resonance study has revealed that below the charge ordering temperature the compound is a mixture of two phases, which are present in different proportions below T_{CO}. The phase fraction of the charge ordered phase increases on cooling between ~220 K and 160 K, while the phase fraction of the charge disordered phase decreases. At low temperatures ($T < 160$ K) the charge ordered to the charge disordered phase ratio is about 4:1, which is in excellent agreement with our previous neutron diffraction results. The exchange phase process revealed reflects the martensitic nature and kinetics of the charge ordering in $Nd_{2/3}Ca_{1/3}MnO_3$. The temperature dependent reverse dc susceptibility shows a clear stepwise behavior which is evident of the weakening of the ferromagnetic correlations and suppression of the double exchange interaction across the charge ordering due to the localization of the charge carriers. It agrees with the temperature dependent resistivity behavior.

Acknowledgment

This work was supported by project TUMOCS. This project has received funding from European Union Horizon 2020 Research and innovation programme under the Marie Sklodowska-Curie Grant agreement no. 645660.

References

[1] J.M.D. Coey, M. Viret, S. von Molnar, Adv. Phys. 48 (1999) 167.
[2] M.B. Salamon, M. Jaime, Rev. Mod. Phys. 73 (2001) 583.
[3] E. Dagotto, T. Hotta, A. Moreo, Phys. Rep. 344 (2001) 1.
[4] M. Uehara, S. Mori, C.H. Chen, S.-W. Cheong, Nature 399 (1999) 560.
[5] A. Moreo, S. Yunoki, E. Dagotto, Science 283 (1999) 2034.
[6] D.E. Cox, P.G. Radaelli, M. Marezio, S.-W. Cheong, Phys. Rev. B 57 (1998) 3305.
[7] A.B. Beznosov, E.L. Fertman, V.A. Desnenko, Low Temp. Phys. 34 (2008) 624.
[8] V. Podzorov, B.G. Kim, V. Kiryukhin, M.E. Gershenson, S.-W. Cheong, Phys. Rev. B 64 (1–4) (2001) 140406.
[9] P.G. Radaelli, R.M. Ibberson, S.-W. Cheong, J.F. Mitchell, Physica B 276–278 (2000) 551.
[10] E. Fertman, D. Sheptyakov, A. Beznosov, V. Desnenko, D. Khalyavin, J. Magn. Magn. Mater. 293 (2005) 787–792.
[11] A. Beznosov, E. Fertman, V. Desnenko, M. Kajňaková, A. Feher, J. Magn. Magn. Mater. 323 (2011) 2380.
[12] E. Fertman, S. Dolya, V. Desnenko, L.A. Pozhar, M. Kajňaková, A. Feher, J. Appl. Phys. 115 (2014) 203906.
[13] V.A. Ivanshin, J. Deisenhofer, H.-A. Krug von Nidda, A. Loidl, A.A. Mukhin, A. M. Balbashov, M.V. Eremin, Phys. Rev. B 61 (2000) 6213.
[14] J. Deisenhofer, B.I. Kochelaev, E. Shilova, A.M. Balbashov, A. Loidl, H.-A. Krug von Nidda, Phys. Rev. B 68 (2003) 214427.
[15] G. Alejandro, M.C.G. Passeggi, D. Vega, C.A. Ramos, M.T. Causa, M. Tovar, R. Senis, Phys. Rev. B 68 (2003) 214429.
[16] A. Pimenov, M. Biberacher, D. Ivannikov, A. Loidl, V. Yu Ivanov, A.A. Mukhin, A. M. Balbashov, Phys. Rev. B 62 (2000) 5685.
[17] M. Farle, Rep. Prog. Phys. 61/7 (1998) 755.
[18] A.I. Tovstolytkin, A.N. Pogorilyi, E.V. Shypil, D.I. Podyalovski, Phys. Met. Metall. 91 (Suppl. 1) (2001) S214.
[19] A.G. Gurevich, G.A. Melkov, Magnetization Oscillations and Waves, CRC Press, Boca Raton, FL, 1996.
[20] A.I. Tovstolytkin, V.V. Dzyublyuk, D.I. Podyalovskii, X. Moya, C. Israel, D. Sánchez, M.E. Vickers, N.D. Mathur, Phys. Rev. B 83 (2011) 184404.
[21] A. Beznosov, V. Desnenko, E. Fertman, C. Ritter, D. Khalyavin, Phys. Rev. B 68 (2003) 054109.
[22] Janhavi P. Joshi, S.V. Dhat, J. Magn. Reson. 168 (2004) 284.
[23] M. Peter, D. Shaltiel, J.H. Wernick, H.J. Williams, J.B. Mock, R.C. Sherwood, Phys. Rev. 126 (1962) 1395.
[24] (a) F.J. Dyson, Phys. Rev. 98 (1955) 249;
(b) G. Feher, A.F. Kip, Phys. Rev. 98 (1955) 337.
[25] C. Rettori, D. Rao, J. Singley, D. Kidwell, S.B. Oseroff, M.T. Causa, J.J. Neumeier, K.J. McClellan, S.-W. Cheong, S. Schultz, Phys. Rev. B 55 (1997) 3083.
[26] A. Shengelaya, Guo-meng Zhao, H. Keller, K.A. Muller, Phys. Rev. Lett. 77 (1996) 5296.
[27] (a) D.L. Huber, M.S. Seehra, J. Phys. Chem. Solids 36 (1975) 723;
(b) M.S. Seehra, R.P. Gupta, Phys. Rev. B 9 (1974) 197.
[28] (a) D.L. Huber, D. Laura-Ccahuana, M. Tovar, M.T. Causa, J. Magn. Magn. Mater. 310 (2007) e604–e606;
(b) S.B. Oseroff, N.O. Moreno, P.G. Pagliuso, C. Rettori, D.L. Huber, J.S. Gardner, J. L. Sarrao, J.D. Thompson, M.T. Causa, G. Alejandro, M. Tovar, B.R. Alascio, J. Appl. Phys. 87 (2000) 5810.
[29] M.T. Causa, M. Tovar, A. Caneiro, F. Prado, G. Ibanez, C.A. Ramos, A. Butera, B. Alascio, X. Obradors, S. Pinol, F. Rivadulla, C. Vazquez-Vazquez, M.A. Lopez-Quintela, J. Rivas, Y. Tokura, S.B. Oseroff, Phys. Rev. B 58 (1998) 3233.
[30] S.B. Oseroff, M. Torikachvili, J. Singley, S. Ali, S.-W. Cheong, S. Schultz, Phys. Rev. B 53 (1996) 6521.
[31] K. Liu, X.W. Wu, K.H. Ahn, T. Sulchek, C.L. Chien, J.Q. Xiao, Phys. Rev. B 54 (1996) 3007.
[32] P.G. Radaelli, R.M. Ibberson, D.N. Argyriou, H. Casalta, K.H. Andersen, S.-W. Cheong, J.F. Mitchell, Phys. Rev. B 63 (2001) 172619.
[33] H.W. Tian, W.T. Zheng, Z.D. Zhao, T. Ding, S.S. Yu, B. Zheng, X.T. Li, F.L. Meng, Q. Jiang, Chem. Phys. Lett. 401 (2005) 585.
[34] J.P. Joshi, K.V. Sarathy, A.K. Sood, S.V. Bhat, C.N.R. Rao, J. Phys.: Condens. Matter 16 (2004) 2869.
[35] J.P. Joshi, R. Gupta, A.K. Sood, S.V. Bhat, A.R. Raju, C.N.R. Rao, Phys. Rev. B 65 (2001) 024410.
[36] F. Rivadulla, M. Freita-Alvite, M.A. López-Quintela, L.E. Hueso, D.R. Miguéns, P. Sande, J. Rivas, J. Appl. Phys. 91 (2002) 785.

UNCORRECTED PROOF